

Testing for similarity of dose response in multi-regional clinical trials

Holger Dette²

Lukas Koletzko²

Frank Bretz¹

¹*Novartis Pharma AG*

²*Ruhr-Universität Bochum*

Abstract

This paper addresses the problem of deciding whether the dose response relationships between subgroups and the full population in a multi-regional trial are similar to each other. Similarity is measured in terms of the maximal deviation between the dose response curves. We consider a parametric framework and develop two powerful bootstrap tests for the similarity between the dose response curves of one subgroup and the full population, and for the similarity between the dose response curves of several subgroups and the full population. We prove the validity of the tests, investigate the finite sample properties by means of a simulation study and finally illustrate the methodology in a case study.

Keywords and Phrases: equivalence testing of curves, subgroup analysis, constrained bootstrap

1 Introduction

A multi-regional clinical trial is a single study carried out simultaneously across various regions under a common protocol to investigate the effect of an investigational drug. Its primary goal is often to draw conclusions about the drug's effect across all the regions participating in the trial. Conducted within the framework of a global drug development program, a multi-regional clinical trial aimed at bridging purposes can facilitate the drug's registration across all involved regions. In recent years, such trials have received increasing attention for their potential to reduce resources by avoiding the need for multiple, regional trials (ICH, 2017). Accordingly, multi-regional clinical trials typically have at least two main objectives: demonstrating the drug's efficacy

within individual regions and comparing study results across regions to confirm that the drug's effects are not influenced by ethnic or other regional factors.

The ICH (2017) guideline on general principles for planning and design of multi-regional clinical trials highlights the importance of identifying intrinsic and/or extrinsic ethnic factors that could impact drug responses in the early stages of drug development, prior to the design of confirmatory multi-regional studies. Consequently, recent early-phase studies, especially those focusing on dose response, are increasingly being conducted across multiple countries or regions (Song et al., 2019). The primary aim of multi-regional dose response studies is to establish the dose response relationship using data from the full (i.e., global) population. Once this primary goal is achieved, it becomes important to evaluate whether the results applicable to the full population can be reliably extended to specific regions. To this end, the dose response relationship observed in any given region should be similar to that of the full population. If significant discrepancies are observed, further investigation into the intrinsic and/or extrinsic ethnic factors affecting these outcomes may be necessary.

Many authors consider the problem of how to choose the subgroup sample sizes in multi-regional confirmatory trials in order to allow observing a consistent treatment effect between a regional subgroup and the full population with acceptable probability (see, among others Liao et al., 2018; Teng et al., 2018; Chiang and Hsiao, 2019). More recently, Yamaguchi and Sugitani (2021) and Kaneko (2023) address the problem of sample size allocation for demonstrating consistency (or similarity) in multi-regional dose finding trials. In particular, Yamaguchi and Sugitani (2021) measure consistency between dose response profiles of a regional subgroup and the global population by the probability that the maximal deviation between the two curves falls below a fixed threshold. In order to facilitate the sample size calculations, Kaneko (2023) restricts the calculation of the maximum deviation to the used dose levels and derives an approximation formula for the proposed consistency probability.

Equivalence tests pursue a similar approach and are a common tool to decide whether parameters of interest such as the area under the curve or the peak concentration of two groups are similar. Here, the null hypothesis is defined as an effect exceeding a given threshold and under the alternative the effect is smaller than this bound. Meanwhile there exist well developed methodology on testing the equivalence of finite dimensional parameters (see, for example Wellek, 2010, and the references therein). While a large body of this literature refers to applications in medicine, in particular pharmacokinetics, equivalence tests have also been used in other areas such as economics, psychology or biology (see, for example, Kim et al., 2019; Lakens and Delacre, 2020; Rose et al., 2018). A common feature of all these references consists in the fact that equivalence refers to finite dimensional (often one-) dimensional parameters, which should be close

with respect to some metric.

The problem of investigating the similarity between curves, however, is far less explored. Cade (2011) and Ostrovski (2022) develop tests for the similarity of quantile curves and power law distributions, respectively. In the context of drug development, Liu et al. (2007, 2009); Gsteiger et al. (2011) and Bretz et al. (2018) develop tests for the similarity between dose response curves of two distinct groups of patients utilizing a parametric model assumption and confidence bands for the difference between the two curves. More recently, Dette et al. (2018); Möllenhoff et al. (2020, 2021) propose more powerful similarity tests based on constrained parametric bootstrap. For a Bayesian approach to the problem we also mention Ollier et al. (2021) and the references therein. A common feature in all these references consists in the fact that parameters or curves corresponding to two different and independent groups are compared.

In this paper, we consider the problem of assessing whether the dose response relationships of one or more (regional) subgroups and the full population are similar from a hypothesis testing point of view. Similar to much of the aforementioned literature, we define a parametric model for the clinical trial data and formulate appropriate statistical hypotheses that capture the similarity problem. We propose powerful parametric bootstrap tests for the similarity between the dose response curves of one subgroup and the full population and for the similarity between the dose response curves of several subgroups and the full population. The validity of these procedures is proved rigorously and the performance is analyzed in various scenarios by means of a simulation study which includes small sample sizes. Finally, we illustrate the use of these tests in a multi-regional dose finding case study. Our work differs from that of Yamaguchi and Sugitani (2021) and Kaneko (2023) with respect to several aspects. First, the dose response functions of the subgroups in our model are not restricted to be identical. In fact, they are allowed to have different parametric forms. Second, our model allows not only for two, but also for more than two subgroups and we also propose a test for simultaneously assessing the similarity between several subgroups and the full population. Third, we compare the dose response curve on the full dose range and not only at the dose levels used in the clinical trial. Fourth, we develop a constrained bootstrap test to obtain critical values and p -values.

The remainder of this paper is organized as follows. In Section 2 we introduce the framework and methodology for assessing similarity of one or several subgroups with the full population. Section 3 and Section 4 are dedicated to a simulation study and numerical example, respectively. We conclude with a discussion in Section 5 and give all mathematical details in the Appendix in Section 6.

2 Assessing similarity of subgroups with the full population

Suppose a dose response trial is conducted with r dose levels d_1, \dots, d_r in the dose range $\mathcal{D} = [d_1, d_r]$, where $d_1 = 0$ denotes the placebo group. Assume that a population of patients can be decomposed into k disjoint subgroups (corresponding to the different regions in a multi-regional clinical trial). Let n_ℓ denote the number of patients belonging to subgroup $\ell = 1, \dots, k$, and denote by $n = n_1 + \dots + n_k$ the total number of patients recruited for the trial. Each patient is randomized to one of the dose levels d_1, \dots, d_r . Let $n_{\ell,j}$ denote the number of patients in subgroup ℓ which are treated at dose level d_j ($j = 1, \dots, r$). Following Bretz et al. (2005), Thomas (2006), Bretz et al. (2018); Möllenhoff et al. (2020); Yamaguchi and Sugitani (2021), we assume that the dose response relationships in each subgroup can be described by a (possibly non-linear) parametric dose response model, say $\mu_\ell(\cdot, \beta_\ell) : \mathcal{D} \rightarrow \mathbb{R}$ with a γ_ℓ -dimensional parameter β_ℓ . We model the response of the i th patient treated with dose d_j in subgroup ℓ as a normal distributed random variable with variance $\sigma_\ell^2 > 0$ and mean $\mu_\ell(d_j, \beta_\ell)$, that is

$$Y_{\ell ij} = \mu_\ell(d_j, \beta_\ell) + \epsilon_{\ell ij}, \quad i = 1, \dots, n_{\ell,j}, \quad j = 1, \dots, r, \quad \ell = 1, \dots, k, \quad (2.1)$$

where $\epsilon_{\ell ij}$ are independent centered normal distributed errors with variance $\sigma_\ell^2 > 0$. This means that we assume the patient responses to be independent. Note that the dose response models μ_ℓ and variances σ_ℓ^2 are allowed to be different for the k different subgroups. We are interested in testing whether the mean effect in a particular subgroup is similar to the mean effect in the full population. For this purpose we model the mean treatment effect in the full population as a weighted average of the regional treatment effects, where the weights represent the share of each region in the global or overall effect. Similar modelling approaches are employed by Bean et al. (2023) and Kaneko (2023) among others. Following these authors we assume that the k subgroup proportions in the full population are known and denote these by p_1, \dots, p_k , where p_ℓ represents the positive proportion of the ℓ th subgroup ($\sum_{\ell=1}^k p_\ell = 1$). We define an overall (population) effect at dose d by

$$\bar{\mu}(d, \beta) := \sum_{\ell=1}^k p_\ell \mu_\ell(d, \beta_\ell), \quad (2.2)$$

where $\beta = (\beta_1^\top, \dots, \beta_k^\top)^\top$ denotes the vector of all parameters in the regression models μ_1, \dots, μ_k corresponding to the different subgroups. With these notations we can investigate the problem of testing similarity between the dose response curves of one or more subgroups and the full population.

2.1 Assessing similarity of one subgroup with the full population

Without loss of generality we assume that the dose response curve of the first subgroup $\ell = 1$ has to be compared with the full population. We will address this problem by estimating the maximum deviation

$$d_\infty := d_\infty(\beta) := \max_{d \in \mathcal{D}} |\mu_1(d, \beta_1) - \bar{\mu}(d, \beta)| \quad (2.3)$$

between the (expected) dose response curve μ_1 in subgroup 1 and the dose response curve $\bar{\mu}$ defined in (2.2). In the literature, maximum deviation distances of the form (2.3) are considered to investigate the similarity of curves from two independent groups, see for example Liu et al. (2009); Gsteiger et al. (2011); Dette et al. (2018); Möllenhoff et al. (2021). In the context of multi-regional clinical trials, Yamaguchi and Sugitani (2021) use this distance to study differences between the dose response curves of a subgroup and the full population consisting of $k = 2$ subgroups.

In order to investigate if the observed dose response relationship of a specific subgroup (here the first one) is sufficiently similar to that of the full population we will develop a test for the hypotheses

$$H_0 : d_\infty \geq \Delta \text{ versus } H_1 : d_\infty < \Delta, \quad (2.4)$$

where $\Delta > 0$ is a given threshold that depends on the clinical relevance in a particular application. Note that rejecting H_0 in (2.4) means to decide that the absolute difference between the dose response curves of the regional subgroup and the full population is smaller than Δ over the whole dose range while keeping the probability for a type 1 error bounded by the significance level, say α .

Remark 2.1. In the special case $k = 2$, the hypotheses in (2.4) reduce to the hypotheses considered in Yamaguchi and Sugitani (2021) (up to a constant factor). Note that in this case $p_2 = 1 - p_1$ and the curve for the full population (2.2) reduces to

$$\bar{\mu}(d, \beta) = p_1 \mu_1(d, \beta_1) + (1 - p_1) \mu_2(d, \beta_2),$$

which yields for the maximum deviation distance in (2.3) the representation

$$d_\infty = (1 - p_1) \max_{d \in \mathcal{D}} |\mu_1(d, \beta_1) - \mu_2(d, \beta_2)|.$$

In this case the alternative hypothesis in (2.4) coincides with statement (10) in Kaneko (2023).

To estimate the unknown maximal deviation d_∞ in (2.3) we use a plug-in estimator defined by

$$\hat{d}_\infty := d_\infty(\hat{\beta}) = \max_{d \in \mathcal{D}} |\mu_1(d, \hat{\beta}_1) - \bar{\mu}(d, \hat{\beta})|, \quad (2.5)$$

where $\hat{\beta} = (\hat{\beta}_1^\top, \dots, \hat{\beta}_k^\top)^\top$ and $\hat{\sigma}^2 = (\hat{\sigma}_1^2, \dots, \hat{\sigma}_k^2)^\top$ are the maximum likelihood estimators (mle) of the parameters $\beta = (\beta_1^\top, \dots, \beta_k^\top)^\top$ and $\sigma^2 = (\sigma_1^2, \dots, \sigma_k^2)^\top$, respectively, maximizing the log-likelihood function

$$\log(L(\beta, \sigma^2)) = - \sum_{\ell=1}^k \sum_{j=1}^r \sum_{i=1}^{n_{\ell,j}} \left\{ \log((2\pi\sigma_\ell^2)^{1/2}) + \frac{1}{2\sigma_\ell^2} (Y_{\ell ij} - \mu_\ell(d_j, \beta_\ell))^2 \right\}. \quad (2.6)$$

We reject the null hypothesis in (2.4) for small values of the statistic \hat{d}_∞ . However, the distribution of \hat{d}_∞ under the null is complicated and critical values are difficult to obtain (see Theorem 6.3 in the Appendix). To address this problem, we propose to use a non-standard constrained parametric bootstrap test for the hypotheses (2.4). The pseudo-code for this procedure is given in Algorithm 1.

Algorithm 1 Constrained parametric bootstrap test for hypotheses (2.4)

- (1) Calculate the mle $(\hat{\beta}, \hat{\sigma}^2)$ and test statistic \hat{d}_∞ in (2.5).
- (2) Calculate a constrained version of the mle of β defined by

$$\hat{\tilde{\beta}} = \begin{cases} \hat{\beta}, & \hat{d}_\infty \geq \Delta \\ \tilde{\beta}, & \hat{d}_\infty < \Delta. \end{cases}$$

where $\tilde{\beta}$ is the mle of β in the set $\{\beta : d_\infty(\beta) = \Delta\}$.

- (3) For $\ell = 1, \dots, k$, $j = 1, \dots, r$, $i = 1, \dots, n_{\ell,j}$ generate bootstrap data

$$Y_{\ell ij}^* = \mu_\ell(d_j, \hat{\tilde{\beta}}) + \epsilon_{\ell ij}^*,$$

where $\epsilon_{\ell ij}^*$ are independent centered normal distributed with variance $\hat{\sigma}_\ell^2$.

- (4) Calculate the mle $\hat{\beta}^*$ from the bootstrap data $\{Y_{\ell ij}^*\}_{\ell=1, \dots, k; j=1, \dots, r; i=1, \dots, n_{\ell,j}}$ and the α -quantile \hat{q}_α^* of the distribution of

$$\hat{d}_\infty^* := d_\infty(\hat{\beta}^*) = \max_{d \in \mathcal{D}} |\mu_1(d, \hat{\beta}_1^*) - \bar{\mu}(d, \hat{\beta}^*)|. \quad (2.7)$$

- (5) Reject the null hypothesis in (2.4), whenever

$$\hat{d}_\infty < \hat{q}_\alpha^*. \quad (2.8)$$

Remark 2.2.

- (a) In practice, the quantile \hat{q}_α^* in Algorithm 1 is simulated by the empirical α -quantile of B realizations of the bootstrap statistic \hat{d}_∞^* in (2.7). More precisely, if $\hat{d}_\infty^{*,(1)}, \dots, \hat{d}_\infty^{*,(B)}$ denote B independent bootstrap copies of \hat{d}_∞^* generated by Algorithm 1, the empirical α -quantile of this sample, say $\hat{q}_\alpha^{*,B}$, is used as an estimate of \hat{q}_α^* . In a similar way we can define a p -value for testing the hypotheses (2.4) by

$$p_\infty := \frac{1}{B} \sum_{b=1}^B \mathbb{1}\{\hat{d}_\infty^{*,(b)} \leq \hat{d}_\infty\}. \quad (2.9)$$

- (b) In Theorem 6.1 in the Appendix we establish the validity of this bootstrap test. For sufficiently large sample sizes the test (2.8) keeps its nominal level α . To be

more precise, consider the set

$$\mathcal{E} = \{d \in \mathcal{D} : |\mu_1(d, \beta_1) - \bar{\mu}(d, \beta)| = d_\infty\},$$

which consists of all dose levels where the (absolute) difference between the two dose response curves is maximal. In most applications the set \mathcal{E} has only one element (see Section 3 for some typical non-linear regression models used in dose response trials) and in such situations the properties of the test can be easily described. If $d_\infty > \Delta$ (we call this region *interior of the null hypothesis in* (2.4)) the probability of rejection converges to 0 for increasing sample sizes. If $d_\infty = \Delta$ (we call this region *boundary of the hypotheses in* (2.4)) the probability of rejection converges to the nominal level α for increasing sample sizes. Moreover, the test (2.8) detects the alternative with a probability converging to 1 with increasing sample size, which means that it is consistent. A rigorous formulation of this result and a discussion of the case where \mathcal{E} consists of more than one point can be found in Theorem 6.1. The finite sample properties of the test are investigated in Section 3.1 by means of a simulation study.

- (c) As pointed out in Remark 2.1, Yamaguchi and Sugitani (2021) and Kaneko (2023) assess the similarity between the dose response curves of one subgroup and the full population consisting of only two subgroups. However, even in this case the testing approach considered in the present paper differs from their method as follows. Yamaguchi and Sugitani (2021) and Kaneko (2023) consider the size of a “consistency” (or “assurance”) probability $\mathbb{P}(\hat{d}_\infty < \Delta)$ which is calculated under the assumption that the two curves are exactly identical. In particular, they do not aim for a control of the probability $\mathbb{P}(\hat{d}_\infty \geq \Delta)$ of a type I error, in contrast to the constrained bootstrap test (2.8). Consequently, in the case of two groups, their test cannot be compared directly with the one proposed in this paper as it is not calibrated at the correct nominal level. For example, Table 6 in Kaneko (2023) has to be interpreted with some care as the different tests under consideration are not calibrated for the same type I error rate.

Remark 2.3. Note that the hypotheses in (2.4) are nested. Recalling the definition of the bootstrap in Algorithm 1 it is easy to see that $\hat{d}_{\infty, \Delta_1}^* \leq \hat{d}_{\infty, \Delta_2}^*$, where $\Delta_1 \leq \Delta_2$ and $\hat{d}_{\infty, \Delta}^*$ denotes the bootstrap statistic (2.7) calculated by Algorithm 1 for the threshold Δ . Consequently, we obtain for the corresponding quantiles the inequality $\hat{q}_{\alpha, \Delta_1}^* \leq \hat{q}_{\alpha, \Delta_2}^*$, and rejecting the null hypothesis in (2.4) by the test (2.8) for $\Delta = \Delta_0$ also yields rejection of the null for all $\Delta > \Delta_0$.

Therefore, by the sequential rejection principle, we may simultaneously test the hy-

potheses in (2.4) for different $\Delta \geq 0$ starting at $\Delta = 0$ and increasing Δ to find the minimum value $\hat{\Delta}_\alpha$ for which H_0 is rejected for the first time. This value could be interpreted as a measure of evidence for similarity with a controlled type I error α .

2.2 Assessing similarity of several subgroups with the full population

In this section we extend the methodology for investigating the similarity of $1 \leq m \leq k$ subgroups with the full population. Without loss of generality we assume that we are interested in dose response curves corresponding to the subgroups $1, \dots, m$ and consider the distance

$$d_{\infty, \infty} := d_{\infty, \infty}(\beta) := \max_{1 \leq i \leq m} \max_{d \in \mathcal{D}} |\mu_i(d, \beta_i) - \bar{\mu}(d, \beta)|. \quad (2.10)$$

In order to establish simultaneously the similarity of the dose response curves in the subgroups $1, \dots, m$ with the dose response curve of the full population we consider the null hypothesis

$$H_0 : d_{\infty, \infty} \geq \Delta \quad \text{versus} \quad H_1 : d_{\infty, \infty} < \Delta \quad (2.11)$$

for a pre-specified threshold $\Delta > 0$. By the intersection-union principle (see, for example, Sonnemann, 2008), it can be tested by applying the test (2.8) from Section 2.1 for each subgroup $i = 1, \dots, m$. The null hypothesis (2.11) is then rejected if and only if all individual tests reject the individual null hypotheses of similarity between the i th curve and the dose response curve of the full population.

However, as tests based on the intersection-union principle can be conservative, we propose an alternative, more powerful test in the following. To this end, recall the definition of the estimators $\hat{\beta}_1, \dots, \hat{\beta}_m$ and $\hat{\beta}$ in Section 2.1. We estimate $d_{\infty, \infty}$ by

$$\hat{d}_{\infty, \infty} := d_{\infty, \infty}(\hat{\beta}) = \max_{1 \leq i \leq m} \max_{d \in \mathcal{D}} |\mu_i(d, \hat{\beta}_i) - \bar{\mu}(d, \hat{\beta})| \quad (2.12)$$

and reject the null hypothesis in (2.11) for small values of $\hat{d}_{\infty, \infty}$. The corresponding quantiles are obtained by the constrained parametric bootstrap test in Algorithm 2, where the decision rule is defined by (2.14). In practice, the quantile $\hat{q}_{\alpha, \infty}^*$ in (2.14) is estimated by the empirical α -quantile of the bootstrap sample $\hat{d}_{\infty, \infty}^{*,(1)}, \dots, \hat{d}_{\infty, \infty}^{*,(B)}$, where for $b = 1, \dots, B$ the quantity $\hat{d}_{\infty, \infty}^{*,(b)}$ is generated by Algorithm 2. The p -value for testing

the hypotheses (2.11) is defined by

$$p_{\infty, \infty} := \frac{1}{B} \sum_{b=1}^B \mathbb{1}\{\hat{d}_{\infty, \infty}^{*, (b)} \leq \hat{d}_{\infty, \infty}\}. \quad (2.13)$$

In Section 6.3 of the Appendix we show that the decision rule (2.14) defines a valid test for the hypotheses (2.11). The finite sample properties of this test are investigated in Section 3.2 by means of a simulation study.

Algorithm 2 Constrained parametric bootstrap test for hypotheses (2.11)

- (1) Calculate the mle $(\hat{\beta}, \hat{\sigma}^2)$ and the test statistic $\hat{d}_{\infty, \infty}$ in (2.12).
- (2) Calculate a constrained version of the mle of β defined by

$$\hat{\tilde{\beta}} = \begin{cases} \hat{\beta}, & \hat{d}_{\infty, \infty} \geq \Delta \\ \tilde{\beta}, & \hat{d}_{\infty, \infty} < \Delta. \end{cases}$$

where $\tilde{\beta}$ is the mle of β in the set $\{\beta : d_{\infty, \infty}(\beta) = \Delta\}$.

- (3) For $\ell = 1, \dots, k$, $j = 1, \dots, r$, $i = 1, \dots, n_{\ell, j}$ generate bootstrap data

$$Y_{\ell ij}^* = \mu_{\ell}(d_j, \hat{\tilde{\beta}}) + \epsilon_{\ell ij}^*,$$

where $\epsilon_{\ell ij}^*$ are independent, centered normal distributed with variance $\hat{\sigma}_{\ell}^2$.

- (4) Calculate the mle $\hat{\beta}^*$ from the bootstrap data $\{Y_{\ell ij}^*\}_{\ell=1, \dots, k; j=1, \dots, r; i=1, \dots, n_{\ell, j}}$ and the α -quantile $\hat{q}_{\alpha, \infty}^*$ of the distribution of

$$\hat{d}_{\infty, \infty}^* := d_{\infty, \infty}(\hat{\beta}^*) = \max_{1 \leq i \leq m} \max_{d \in \mathcal{D}} |\mu_i(d, \hat{\beta}_i^*) - \bar{\mu}(d, \hat{\beta}^*)|.$$

- (5) Reject the null hypothesis in (2.11), whenever

$$\hat{d}_{\infty, \infty} < \hat{q}_{\alpha, \infty}^*. \quad (2.14)$$

3 Finite sample properties

In this section we investigate the finite sample performance of the bootstrap procedures defined in Algorithm 1 and Algorithm 2 by means of a simulation study. The constrained maximum likelihood estimators $\hat{\tilde{\beta}}$ (see step (2) in both Algorithms) are computed with the `auglag` function provided by the `alabama` package in R.

3.1 Assessing similarity of one subgroup with the full population

Our simulation setup is inspired by a multi-regional clinical trial design for a Phase II dose finding study for an anti-anxiety drug first considered in Pinheiro et al. (2006) and subsequently investigated in Yamaguchi and Sugitani (2021) and Kaneko (2023). We consider a population with $k = 3$ regional subgroups, where $\ell = 1, 2, 3$ denote the Japanese, North American, and European regions, respectively, and assume the proportions $p_1 = 0.1$, $p_2 = 0.3$ and $p_3 = 0.6$. We test for similarity between the full population and the Japanese subgroup ($\ell = 1$) using the test (2.8) in Algorithm 1 for the hypotheses (2.4). The dose range is $\mathcal{D} = [0, 150]$ (in mg) and we consider six dose levels 0, 10, 25, 50, 100 and 150. We fix a total sample size of $n = 450$ patients, but consider two cases for the sample size allocations across subgroups:

$$n_1 = 150, \quad n_2 = 150, \quad n_3 = 150 \quad (3.1)$$

$$n_1 = 66, \quad n_2 = 192, \quad n_3 = 192 \quad (3.2)$$

The motivation for these two scenarios is to investigate a balanced patient allocation in scenario (3.1) and a more realistic allocation in scenario (3.2) where the proportion of Japanese patients in the trial is smaller than those of the two other regions. In both scenarios (3.1) and (3.2) we investigate two choices for the number of patients allocated at each dose level

$\mathcal{D}_=$: In each subgroup the same number of patients is treated at each dose level 0, 10, 25, 50, 100, and 150.

$\mathcal{D}_{\neq}^{(1)}$: In scenario (3.1) in each subgroup 35, 20, 20, 20, 20 and 35 patients are treated at dose levels 0, 10, 25, 50, 100 and 150, respectively.

$\mathcal{D}_{\neq}^{(2)}$: In scenario (3.2) in the first subgroup 15, 9, 9, 9, 9 and 15 are treated at dose levels 0, 10, 25, 50, 100 and 150, respectively, whereas in the other two subgroups 46, 25, 25, 25, 25 and 46 patients are treated at those dose levels.

For the dose response curves in the three subgroups we consider E-max curves defined by

$$E_0 + \frac{E_{\max} \cdot d^h}{d^h + ED_{50}^h}, \quad (3.3)$$

where E_0 represents the placebo effect of the drug (obtained for $d = 0$), E_{\max} denotes the maximum effect, ED_{50} is the dose which produces half of E_{\max} and h denotes the slope (or Hill-) parameter which controls the steepness of the dose response curve. The

errors in model (2.1) are assumed to be centered normal distributed with standard deviation $\sigma_\ell = 0.1$ ($\ell = 1, 2, 3$). For the mean functions we distinguish three scenarios (A), (B) and (C) (see Table 1),

	μ_1	μ_2	μ_3
(A)	$(0, E_{max}, ED_{50}, 1)$	$(0, 0.46, 26, 1)$	$(0, 0.46, 25.5, 1)$
(B)	$(0, E_{max}, 25, h)$	$(0, 0.46, 26, 1)$	$(0, 0.46, 25.5, 1)$
(C)	$(0, E_{max}, ED_{50}, h)$	$(0, 0.46, 27, 2.5)$	$(0, 0.46, 26.5, 2.5)$

Table 1: *Parameters $(E_0, E_{max}, ED_{50}, h)$ in the E-Max models μ_1 , μ_2 and μ_3 (see equation (3.3)). The non-specified parameters for μ_1 are defined in the simulation.*

where the parameters E_{max} , ED_{50} and h of the first curve are varied for simulating the rejection probability of the Algorithms in the interior, on the boundary of the null hypothesis and under the alternative. The choice of these parameters is inspired by the (single) E-Max candidate dose response model considered in Yamaguchi and Sugitani (2021) who set the parameters as $E_0 = 0$, $E_{max} = 0.46$, $ED_{50} = 25$ and $h = 1$. In scenario (A) and (B) the curve for the first subgroup is chosen to deviate more and more from this reference dose response model as we vary the parameters ED_{50} , respectively h . Scenario (C) is added to also investigate the case, where both the ED_{50} and Hill-coefficient of the Japanese curve vary simultaneously. Note that in all three scenarios (A), (B) and (C) the curves for the North American and European subgroup are chosen to be very close to each other as this would generally be expected in practice. To reflect reality, the E_{max} parameter of the Japanese curve is also chosen very similar to the one for the North American and European subgroup (approximately 0.46) throughout all parameter choices. The curves corresponding to the different subgroups are displayed in Figure 1, where we show several curves for the first subgroup.

The rejection probabilities of the test (2.8) are displayed in Table 2, 3 and 4 for the scenarios (A), (B) and (C), respectively. Note that the E_0 -coefficients are estimated in all scenarios. We begin with a discussion of the case (A) in Table 2. Here we consider two cases: first, we assume the Hill-parameters of the curves to be known, resulting in 9 parameters to be estimated overall (three for each curve); second we also estimate these parameters, yielding 12 unknown parameters. The numbers in brackets represent the results for the model in (A) where the Hill-coefficient is assumed to be known ($h = 1$) and is not estimated. We observe that the test keeps its nominal level $\alpha = 10\%$ whenever $d_\infty \geq \Delta = 0.1$ and has reasonable power for $d_\infty < \Delta = 0.1$. When all four parameters of the models are estimated the test (2.8) is conservative: even at the boundary $d_\infty = \Delta$ the level is smaller than α . On the other hand, if the Hill-coefficients in all three models are assumed to be known, the simulated level at the boundary is close to $\alpha = 10\%$. Fixing the Hill-parameter yields also a significant

improvement in power. For example, under the alternative determined by the Japanese curve with $ED_{50} = 10$ and $E_{max} = 0.42$ (third row) the power of the test more than doubles in all four dosing scenarios, if we assume the Hill-coefficients of the curves to be known. For instance, for the equidistant design $\mathcal{D}_=$ the power improves from 0.317 to 0.672. A comparison of the sample size allocations to the different dose levels shows that an equal allocation $\mathcal{D}_=$ yields a more powerful test than the designs \mathcal{D}_{\neq} . Similarly, using the equal sample sizes (3.1) for the populations yields a more powerful test than using a non-uniform design as (3.2).

Next, we discuss the results for scenario (B) and (C), where all four parameters in the three models are estimated. The rejection probabilities for scenario (B) are displayed in Table 3. Again, the test (2.8) keeps its nominal level $\alpha = 10\%$. Note that in this scenario there are two cases corresponding to the boundary $d_{\infty} = \Delta = 0.1$ and the quality of the approximation is different in these cases. In the case $h = 3.5$ and $E_{max} = 0.40$ the approximation of the nominal level at the boundary of the hypotheses is much more accurate as in the case $h = 0.3$ and $E_{max} = 0.47$, in particular for equal sample sizes of the populations (as specified in (3.1)) and a corresponding equidistant design. Similarly to scenario (A) power is improved by equal sizes for the populations and equal sample sizes at the different dose levels. For some cases the results can be compared with the results in Table 2. For example, for $h = 1.5$ and $E_{max} = 0.43$ we obtain $d_{\infty} = 0.04$, which corresponds to the case $ED_{50} = 15$ and $E_{max} = 0.44$ in Table 2. In this case the alternative in scenario (B) is easier to detect than the alternative in (A), although both cases yield a maximal deviation $d_{\infty} = 0.04$. These observations indicate that the power of the test (2.8) is not completely determined by the distance d_{∞} but also depends on the properties of the curves. The results in Table 4 for the scenario (C) show a similar picture as for cases (A) and (B) and confirm our findings. We mention again that, in all three scenarios, the test (generally) performs best if the sample sizes for the subgroups are identical and the patients are allocated uniformly to the different dose levels. These results suggest that, in order to improve the power of the equivalence test (2.8), the best strategy is to choose the subgroup (and dose group) sizes as uniform as possible. However, we emphasize that this rule of thumb is only applicable, if the variances in all groups and all dose levels are similar.

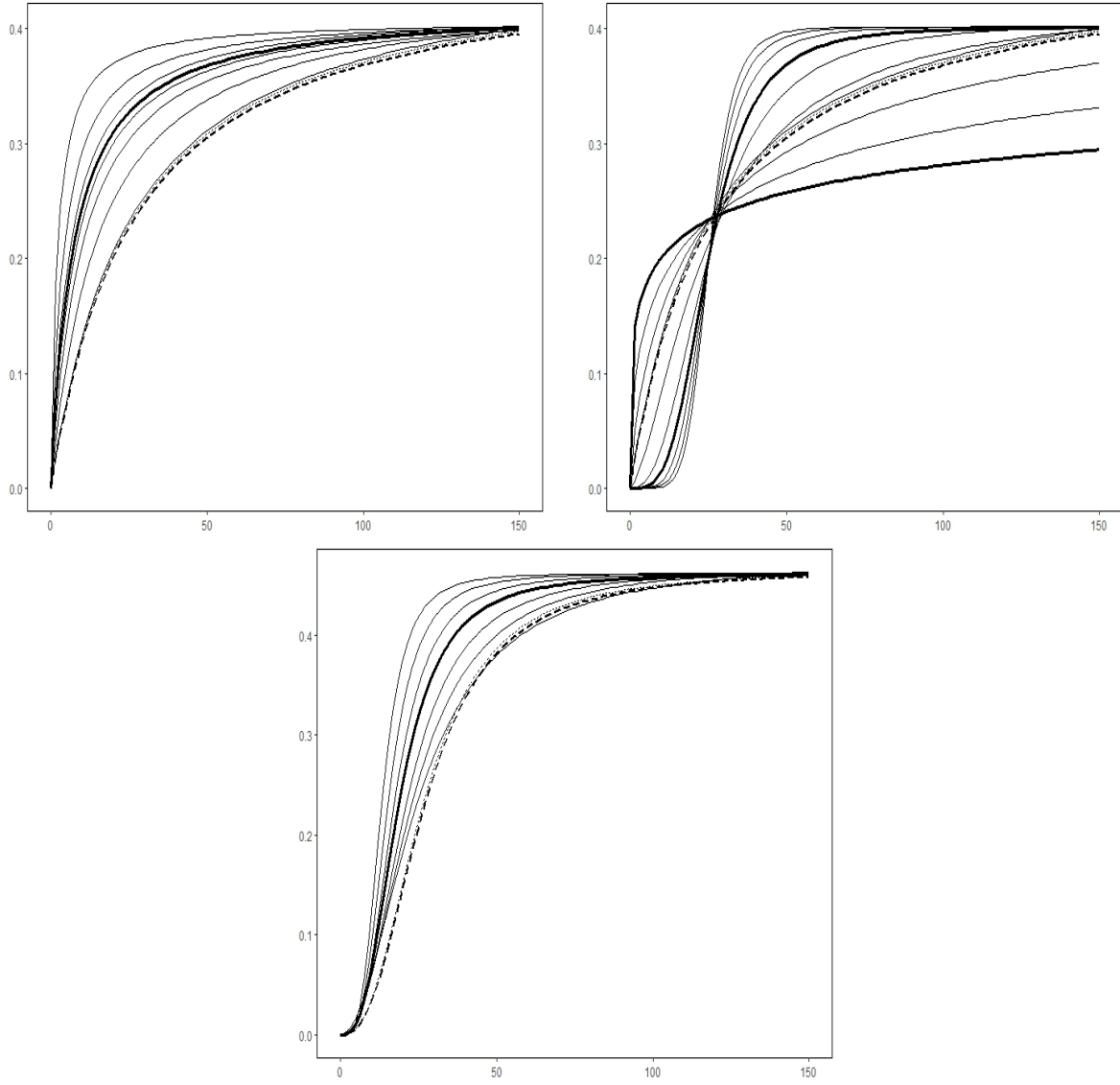


Figure 1: *The dose response curves considered in the simulation study. Top row: scenario (A) (left) and scenario (B) (right); bottom row: scenario (C). The (different) solid curves correspond to the first subgroup (for various parameters E_{\max} , ED_{50} and h), whereas the dashed and dotted curve correspond to the second and third subgroup, respectively. The thick solid curves satisfy $d_{\infty} = \Delta = 0.1$ and mark the boundary of the null hypothesis set.*

(ED_{50}, E_{max})	d_{∞}	(3.1)		(3.2)	
		$\mathcal{D}_{=}$	$\mathcal{D}_{\neq}^{(1)}$	$\mathcal{D}_{=}$	$\mathcal{D}_{\neq}^{(2)}$
(25, 0.47)	0.00	0.996 (1.000)	0.994 (1.000)	0.954 (0.986)	0.952 (0.996)
(15, 0.44)	0.04	0.884 (0.990)	0.838 (0.972)	0.704 (0.898)	0.670 (0.892)
(10, 0.42)	0.07	0.317 (0.672)	0.278 (0.590)	0.224 (0.450)	0.198 (0.448)
(8, 0.42)	0.09	0.077 (0.228)	0.078 (0.206)	0.090 (0.200)	0.062 (0.192)
(7, 0.42)	0.10	0.027 (0.094)	0.034 (0.082)	0.030 (0.092)	0.022 (0.098)
(6, 0.42)	0.11	0.007 (0.018)	0.014 (0.022)	0.014 (0.020)	0.010 (0.046)
(4, 0.41)	0.14	0.000 (0.000)	0.000 (0.002)	0.000 (0.000)	0.002 (0.000)
(2, 0.40)	0.19	0.000 (0.000)	0.000 (0.000)	0.000 (0.000)	0.000 (0.000)

Table 2: *Scenario (A): Simulated rejection probabilities of the test (2.8) in Algorithm 1 for subgroup standard deviation $\sigma_{\ell} = 0.1$, significance level $\alpha = 0.1$ and equivalence threshold $\Delta = 0.1$ for different sample sizes of the subgroups and different dose group sizes. Results in brackets are obtained without estimation of the Hill-parameters of the curves.*

(h, E_{max})	d_{∞}	(3.1)		(3.2)	
		$\mathcal{D}_{=}$	$\mathcal{D}_{\neq}^{(1)}$	$\mathcal{D}_{=}$	$\mathcal{D}_{\neq}^{(2)}$
(0.3, 0.47)	0.10	0.068	0.072	0.072	0.09
(0.5, 0.47)	0.06	0.59	0.550	0.420	0.454
(0.75, 0.47)	0.03	0.958	0.954	0.864	0.848
(1, 0.47)	0.00	0.994	0.998	0.950	0.944
(1.5, 0.43)	0.04	0.978	0.944	0.828	0.842
(2.5, 0.41)	0.08	0.440	0.408	0.322	0.292
(3.5, 0.40)	0.10	0.102	0.092	0.08	0.078
(4.5, 0.40)	0.12	0.022	0.036	0.044	0.042
(5.5, 0.40)	0.13	0.004	0.020	0.018	0.020
(6.5, 0.40)	0.14	0.000	0.008	0.016	0.022

Table 3: *Scenario (B): Simulated rejection probabilities of the test (2.8) in Algorithm 1 for subgroup standard deviation $\sigma_{\ell} = 0.1$, significance level $\alpha = 0.1$ and equivalence threshold $\Delta = 0.1$ for different sample sizes of the subgroups and different dose group sizes.*

(h, ED_{50}, E_{max})	d_{∞}	(3.1)		(3.2)	
		$\mathcal{D}_{=}$	$\mathcal{D}_{\neq}^{(1)}$	$\mathcal{D}_{=}$	$\mathcal{D}_{\neq}^{(2)}$
(2, 25, 0.47)	0.03	0.966	0.946	0.852	0.782
(2.25, 23, 0.47)	0.04	0.935	0.850	0.760	0.696
(2.5, 21, 0.46)	0.06	0.646	0.550	0.394	0.348
(2.75, 18.5, 0.46)	0.10	0.072	0.052	0.058	0.042
(3, 17, 0.46)	0.13	0.004	0.008	0.008	0.006
(3.25, 15, 0.46)	0.16	0.000	0.000	0.000	0.000
(3.5, 13, 0.46)	0.20	0.000	0.000	0.000	0.000

Table 4: *Scenario (C): Simulated rejection probabilities of the test (2.8) in Algorithm 1 for subgroup standard deviation $\sigma_{\ell} = 0.1$, significance level $\alpha = 0.1$ and equivalence threshold $\Delta = 0.1$ for different sample sizes of the subgroups and different dose group sizes.*

3.2 Assessing similarity of all subgroups with a full population

In this section we investigate the finite sample performance of the bootstrap procedure defined in Algorithm 2 for the same three scenarios (A), (B), (C) and dose designs defined in Section 3.1. We consider the case where all three subgroups are compared with the full population, i.e $m = k = 3$. The results of the simulation are displayed in Tables 5-7.

The simulation results for Algorithm 2 are in line with its theoretical validity established in Theorem 6.2, that is, the test keeps its nominal level $\alpha = 10\%$ under the null hypothesis $d_{\infty, \infty} \geq \Delta = 0.1$ and has acceptable power under the alternative hypothesis. Overall, the finite sample performance of Algorithm 2 in the three considered scenarios is very similar to that of Algorithm 1 presented in the previous section. We therefore omit a more detailed discussion for the sake of brevity.

		(3.1)		(3.2)	
(ED_{50}, E_{max})	$d_{\infty, \infty}$	$\mathcal{D}_=$	$\mathcal{D}_{\neq}^{(1)}$	$\mathcal{D}_=$	$\mathcal{D}_{\neq}^{(2)}$
(25, 0.47)	0.00	0.998 (1.000)	0.994 (1.000)	0.962 (0.986)	0.950 (1.000)
(15, 0.44)	0.04	0.872 (0.992)	0.832 (0.982)	0.690 (0.940)	0.664 (0.918)
(10, 0.42)	0.07	0.344 (0.696)	0.250 (0.624)	0.258 (0.464)	0.232 (0.412)
(8, 0.42)	0.09	0.090 (0.252)	0.078 (0.218)	0.072 (0.166)	0.062 (0.184)
(7, 0.42)	0.10	0.030 (0.100)	0.038 (0.102)	0.022 (0.072)	0.028 (0.100)
(6, 0.42)	0.12	0.006 (0.016)	0.008 (0.020)	0.006 (0.016)	0.008 (0.032)
(4, 0.41)	0.15	0.000 (0.000)	0.000 (0.000)	0.000 (0.004)	0.000 (0.004)
(2, 0.40)	0.19	0.000 (0.000)	0.000 (0.000)	0.000 (0.000)	0.000 (0.000)

Table 5: *Scenario (A): Simulated rejection probabilities of the test (2.14) in Algorithm 2 for subgroup standard deviation $\sigma_\ell = 0.1$, significance level $\alpha = 0.1$ and equivalence threshold $\Delta = 0.1$ for different sample sizes of the subgroups and different dose group sizes. Results in brackets are obtained without estimation of the Hill-parameters of the curves.*

		(3.1)		(3.2)	
(h, E_{max})	$d_{\infty, \infty}$	$\mathcal{D}_=$	$\mathcal{D}_{\neq}^{(1)}$	$\mathcal{D}_=$	$\mathcal{D}_{\neq}^{(2)}$
(0.3, 0.47)	0.10	0.038	0.044	0.036	0.060
(0.5, 0.47)	0.06	0.454	0.460	0.384	0.368
(0.75, 0.47)	0.03	0.930	0.890	0.802	0.762
(1, 0.47)	0.00	0.992	0.986	0.926	0.936
(1.5, 0.43)	0.04	0.966	0.922	0.804	0.806
(2.5, 0.41)	0.08	0.262	0.278	0.212	0.244
(3.5, 0.40)	0.10	0.052	0.060	0.072	0.084
(4.5, 0.40)	0.12	0.020	0.008	0.020	0.032
(5.5, 0.40)	0.13	0.002	0.006	0.008	0.026
(6.5, 0.40)	0.14	0.002	0.004	0.012	0.016

Table 6: *Scenario (B): Simulated rejection probabilities of the test (2.14) in Algorithm 2 for subgroup standard deviation $\sigma_\ell = 0.1$, significance level $\alpha = 0.1$ and equivalence threshold $\Delta = 0.1$ for different sample sizes of the subgroups and different dose group sizes.*

(h, ED_{50}, E_{max})	$d_{\infty, \infty}$	(3.1)		(3.2)	
		$\mathcal{D}_=$	$\mathcal{D}_{\neq}^{(1)}$	$\mathcal{D}_=$	$\mathcal{D}_{\neq}^{(2)}$
(2, 25, 0.47)	0.03	0.952	0.928	0.868	0.802
(2.25, 23, 0.47)	0.04	0.916	0.850	0.754	0.722
(2.5, 21, 0.46)	0.06	0.604	0.538	0.462	0.354
(2.75, 18.5, 0.46)	0.10	0.074	0.056	0.062	0.050
(3, 17, 0.46)	0.13	0.000	0.004	0.010	0.010
(3.25, 15, 0.46)	0.16	0.000	0.000	0.000	0.000
(3.5, 13, 0.46)	0.20	0.000	0.000	0.000	0.000

Table 7: *Scenario (C): Simulated rejection probabilities of the test (2.14) in Algorithm 2 for subgroup standard deviation $\sigma_\ell = 0.1$, significance level $\alpha = 0.1$ and equivalence threshold $\Delta = 0.1$ for different sample sizes of the subgroups and different dose group sizes.*

4 Numerical example

In this section we illustrate the proposed methodology analyzing a multi-regional dose finding trial example. We apply the methodology to the data from the dose finding study described in Section 7 of Biesheuvel and Hothorn (2002) and re-analyzed in Dette et al. (2018). The original data set is available in the R package `DoseFinding` (see Bornkamp et al. (2015)). In this study 369 patients with Irritable Bowel Syndrome (IBS) are investigated at five blinded doses 0 (placebo), 1, 2, 3 and 4 with the primary endpoint being a baseline-adjusted abdominal pain score. The different dose groups in the study are of approximately equal size.

Since no information about the region is available in the original dataset, we randomly allocated the 369 patients to one of three regional subgroups (i.e., Japan, North America, and Europe) with probabilities $p_1 = 1/7$, $p_2 = 3/7$ and $p_3 = 3/7$, respectively. Accordingly, we also use these proportions in the definition of the overall population dose response function (2.2). The resulting data set consists of 58 Japanese, 141 North American and 170 European patients. We assume that the subgroup dose response functions are given by three-parametric E-Max models as defined in (3.3), where we assume a fixed Hill-coefficient $h = 1$. The fitted dose response curves of the subgroups based on the maximum likelihood estimates are then given by

$$\mu_J(d) = 0.38 + \frac{0.66 \cdot d}{d + 3.94} \quad , \quad \mu_A(d) = 0.00 + \frac{0.68 \cdot d}{d + 1.41} \quad , \quad \mu_E(d) = -0.03 + \frac{0.90 \cdot d}{d + 0.85} ,$$

representing the Japanese, North American and European subgroup, respectively. These subgroup curves, together with the corresponding dose response data, are displayed in

Figure 2 which also shows the estimated effects at the dose levels with corresponding 90 % confidence intervals. In particular, the subgroup error variances are estimated as $\hat{\sigma}_J^2 = 0.58$, $\hat{\sigma}_A^2 = 0.67$ and $\hat{\sigma}_E^2 = 0.72$. Figure 3 presents a more detailed comparison between the three curves and the average population curve.

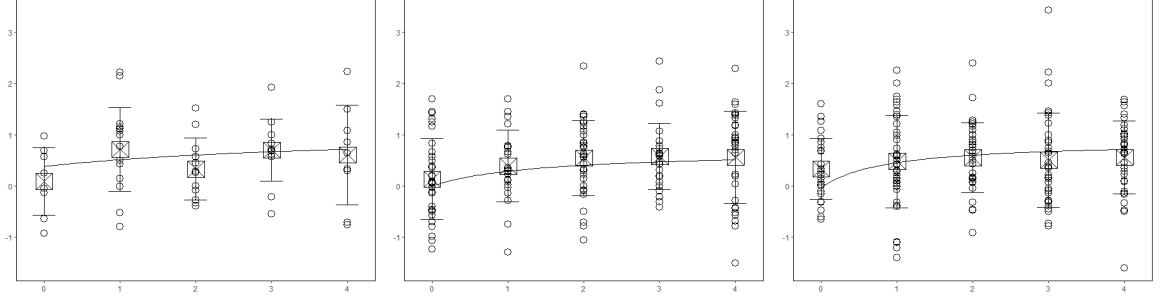


Figure 2: The dose response data and fitted E-Max curves for the Japanese (left), North American (middle) and European (right) subgroups in the trial. Circles represent responses, boxes represent the mean of the responses of a given dose group and bars denote 90 % confidence intervals for the corresponding means.

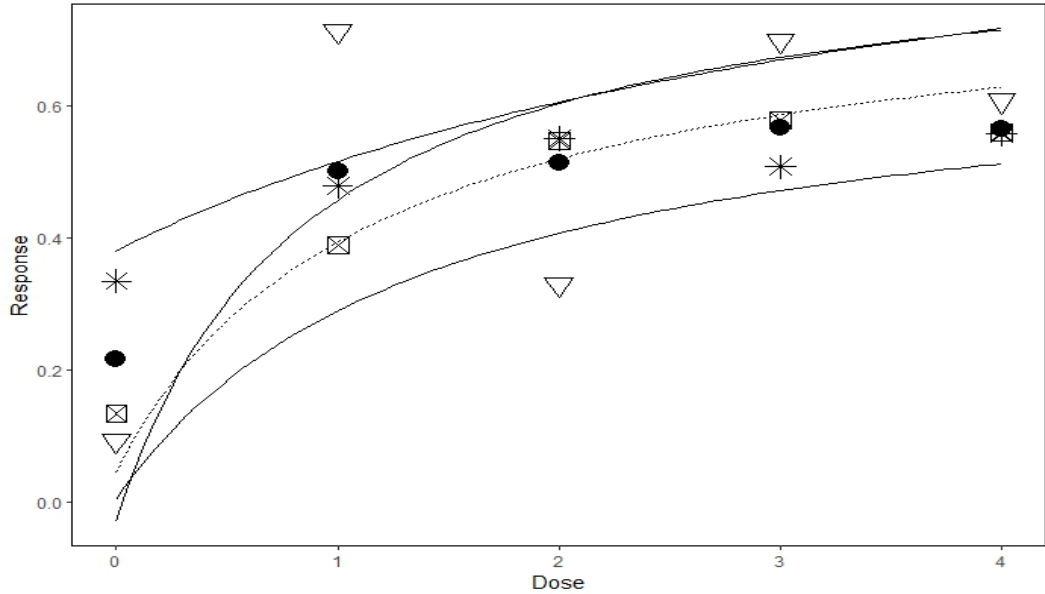


Figure 3: The fitted subgroup (solid) and full population (dotted) dose response curves based on the simulated dataset in the case study. The top, middle and bottom solid curve correspond to the Japanese, European and North American subgroup, respectively. Means: ∇ = Japan, $*$ = Europe, \boxtimes = North America, \bullet = Population.

We now investigate the similarity of subgroup and population dose response curves using Algorithm 1 and Algorithm 2. We use the subscripts “J” (Japan), “A” (North America) and “E” (Europe) to clarify which subgroup is compared to the full popu-

lation. Throughout this section we fix the similarity threshold as $\Delta = 0.4$ and the bootstrap quantiles are calculated by $B = 1000$ bootstrap replications.

First, we test similarity of the European subgroup with the full population by the test (2.8) in Algorithm 1. The corresponding test statistic, i.e the maximum absolute deviation between the estimated European curve and estimated population curve, is $\hat{d}_{\infty,E} = 0.087$. The bootstrap quantile (see step (4) in Algorithm 1) for $\Delta = 0.4$ and $\alpha = 0.05$ (0.1) is $\hat{q}_{\alpha,E}^* = 0.086$ (0.113). We observe that $\hat{d}_{\infty,E} = 0.087 > 0.086 = \hat{q}_{0.05,E}^*$. Thus, the null hypothesis (2.4) cannot be rejected at significance level $\alpha = 0.05$. However, since $\hat{d}_{\infty,E} = 0.087 < 0.113 = \hat{q}_{0.1,E}^*$ we can claim the dose response curves of the European subgroup and the overall population to be similar, that is $d_{\infty,E} < \Delta = 0.4$, at significance level $\alpha = 0.1$. Alternatively, we can compute the corresponding p -value in (2.9). By assessing similarity to the European subgroup for $\Delta = 0.4$ we obtain $p_{\infty,E} = 0.067$ which is smaller than 0.1 but bigger than 0.05.

Next, we apply the test (2.8) in Algorithm 1 to assess whether the dose response curves of the Japanese, respectively, North American region and the full population are similar. The corresponding test statistics are given by $\hat{d}_{\infty,J} = 0.337$ and $\hat{d}_{\infty,A} = 0.116$ and the bootstrap quantiles for the fixed threshold Δ and significance levels $\alpha = 0.05$ (0.1) are $\hat{q}_{\alpha,J}^* = 0.150$ (0.208) and $\hat{q}_{\alpha,A}^* = 0.042$ (0.057). Therefore, at both significance levels, we do not claim the dose response relationship of the Japanese and North American subgroup to be similar to the full population, since each test statistic exceeds the corresponding quantile. Again, we come to the same conclusion by calculating the p -values of the corresponding tests which are given by $p_{\infty,J} = 0.156$ and $p_{\infty,A} = 0.138$.

Whether the subgroups are tested individually with Algorithm 1 or simultaneously with Algorithm 2 depends on the practitioners priorities. Individual tests with Algorithm 1 allow for a more refined understanding of the subgroup similarities as some subgroup dose response curves might be similar to the population curve whereas others are not. However, if Algorithm 1 is applied repeatedly, the significance level α might have to be reduced in each test in order to control the overall type 1 error rate which may yield conservative tests. Applying Algorithm 2 once instead avoids the multiple testing problem on the one hand, but on the other hand only allows investigating if all considered subgroups are similar to the full population.

We now exemplarily test for similarity of all three subgroups with the full population simultaneously using the test (2.14) in Algorithm 2. The corresponding test statistic is calculated as $\hat{d}_{\infty,\infty} = 0.337$ which is the maximum of the three individual test statistics $\hat{d}_{\infty,J}$, $\hat{d}_{\infty,A}$ and $\hat{d}_{\infty,E}$ and coincides with $\hat{d}_{\infty,J}$. The bootstrap quantile for $\Delta = 0.4$ (see step (4) of Algorithm 2) is estimated as $\hat{q}_{\alpha,\infty}^* = 0.189$ (0.235). The p -value at $\Delta = 0.4$

(see (2.13)) is given by $p_{\infty,\infty} = 0.201$. Hence we do not claim that all subgroup dose response functions are similar to the dose response function of the full population.

Figure 4 shows the p -values of the two tests in relation to the equivalence threshold Δ varying in the interval $[0, 1]$. As one might expect (see also Remark 2.3), larger thresholds Δ generally yield smaller p -values and thus a higher chance of rejecting the null hypothesis stating “no similarity” at any given significance level. For example, if Δ is close to one, the p -values are nearly zero. This illustrates the general fact that, for a large enough threshold Δ , any subgroup dose response curve(s) can be claimed similar to the population curve. However, clearly, the larger the threshold Δ the less meaning any such claim will carry for practical purposes.

Observing Figure 4 one may wonder why the p -values stay (approximately) constant for thresholds below the corresponding test statistic of the performed test (see, exemplarily, the dotted line in the right panel of Figure 4). We note that this is a consequence of the definition of the constrained mle defined in step (2) of both Algorithms. If the test statistic exceeds the similarity threshold Δ the bootstrap data is always generated from the unconstrained mle which does not depend on Δ . Consequently, the p -values produced for such thresholds will be (approximately) the same.

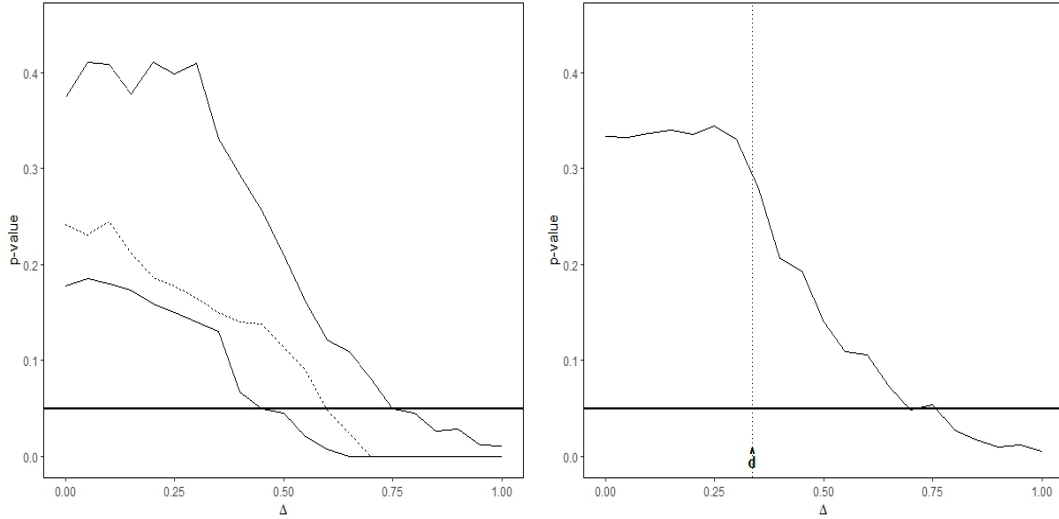


Figure 4: *Left panel: p -values of the test (2.8) in Algorithm 1 assessing similarity between the Japanese (top solid), North American (dotted) and European (bottom solid) subgroup and the full population for different choices of the threshold Δ . Right panel: p -values of the test (2.14) in Algorithm 2 assessing similarity between all three subgroups and the full population for different choices of the threshold Δ . The horizontal solid line marks a p -value of 0.05. The vertical dotted line in the right graphic marks the value of the test statistic $\hat{d}_{\infty,\infty}$.*

5 Conclusions and future research

In this paper, we develop inference tools for assessing the similarity between dose response curves of one or several subgroups and the full population in multi-regional clinical trials. Our approach is based on a statistical test for the null hypothesis that the maximum deviation between the dose response curves is larger than a given threshold Δ . Thus rejection means that the curves of the subgroups deviate by at most Δ from the dose response curve corresponding to the full population over the full dose range. Critical values are determined by a novel parametric bootstrap under a constraint on the parameters such that the null hypothesis is satisfied. An essential ingredient of our approach is the specification of the threshold Δ , which has to be carefully discussed for each application with the clinical team. Alternatively, our approach can be used to define a measure of evidence for similarity with a controlled type I error rate, as pointed out in Remark 2.3.

Our main focus in this paper is on the maximum deviation between the curves, which makes the definition and interpretation of the threshold relatively easy. However, other measures such as the area between the curves might also be useful in applications, and an interesting problem of future research is to extend our approach to such distances. A further important direction of future research is to extend our approach to situations, where the proportions p_ℓ of the subgroups are not known (as assumed in this paper) and have to be estimated from the data. In this case it is not reasonable to work with deterministic sample sizes n_ℓ for the subgroups and patients have to be randomly selected from the full population for the trial. We expect that the methodology can be extended to such situations. Finally, in contrast to many publications on dose finding in multi-regional trials, we did not include a model-selection step via, for example, MCP-Mod (Bretz et al., 2005) in our methodology, but worked with pre-selected dose response models for the subgroups from the beginning. We also look forward to generalize our results to account for model uncertainty in the future.

Acknowledgements: This research is supported by the European Union through the European Joint Programme on Rare Diseases under the European Union’s Horizon 2020 Research and Innovation Programme Grant Agreement Number 825575 and by the Deutsche Forschungsgemeinschaft (DFG, German Research Foundation) – Project-ID 499552394 – SFB 1597.

6 Appendix

6.1 Basic assumptions and main statements

In this section, we provide details about the validity of the two tests (2.8) and (2.14) for the hypotheses (2.4) and (2.11). We begin stating several assumptions that are required for all theoretical results in this paper.

Assumption 1: The k dose response functions $\mu_1(\cdot, \beta_1), \dots, \mu_k(\cdot, \beta_k)$ depend on unknown parameter vectors $\beta_\ell \in \mathbb{R}^{\gamma_\ell}$, $\ell = 1, \dots, k$. We define $\gamma = \sum_{\ell=1}^k \gamma_\ell$ and summarize these unknown vectors in a single vector $\beta = (\beta_1^\top, \dots, \beta_k^\top)^\top$ which belongs to the compact parameter space $\mathcal{B} \subseteq \mathbb{R}^\gamma$.

Assumption 2: For $\ell = 1, \dots, k$ the subgroup dose response function $\mu_\ell(d, \beta_\ell)$ is three times continuously differentiable with respect to β_ℓ and d .

Assumption 3: For $\ell = 1, \dots, k$ we have $n_\ell/n \rightarrow \kappa_\ell \in (0, 1)$ and $n_{\ell,j}/n_\ell \rightarrow \kappa_{\ell,j} \in (0, 1)$ for $j = 1, \dots, r$ as $n_\ell \rightarrow \infty$.

For a statement of our first main result we introduce the random variable

$$T := \max \left\{ \max_{d \in \mathcal{E}^+} G(d), \max_{d \in \mathcal{E}^-} -G(d) \right\}, \quad (5.1)$$

where $\mathcal{E}^\pm := \{d \in \mathcal{D} : \mu_1(d, \beta_1) - \bar{\mu}(d, \beta) = \pm d_\infty\}$, the process $G = \{G(d)\}_{d \in \mathcal{D}}$ is defined by

$$G(d) := \left(\frac{\partial(\mu_1(d, b_1) - \bar{\mu}(d, b))}{\partial b} \right)^T \Big|_{b=\beta} Z, \quad d \in \mathcal{D} \quad (5.2)$$

and Z is a centered γ -dimensional normal distributed random variable with block diagonal covariance matrix

$$\Sigma = \text{diag}(\frac{1}{\kappa_1} \Sigma_1^{-1}, \dots, \frac{1}{\kappa_k} \Sigma_k^{-1}) \in \mathbb{R}^{\gamma \times \gamma}, \quad (5.3)$$

where

$$\Sigma_\ell = \frac{1}{\sigma_\ell^2} \sum_{j=1}^r \kappa_{\ell,j} \left(\frac{\partial}{\partial b_\ell} \mu_\ell(d_j, b_\ell) \Big|_{b_\ell=\beta_\ell} \right) \left(\frac{\partial}{\partial b_\ell} \mu_\ell(d_j, b_\ell) \Big|_{b_\ell=\beta_\ell} \right)^\top \in \mathbb{R}^{\gamma_\ell \times \gamma_\ell}, \quad \ell = 1, \dots, k.$$

Theorem 6.1. *Let Assumptions 1-3 be satisfied and assume that the random variable T in (5.1) has a continuous distribution function. Furthermore, let $\alpha \in (0, 1)$ be small enough, such that the α -quantile of T is negative. Then the test defined by (2.8) for the hypotheses (2.4) is consistent and has asymptotic level α . More precisely,*

(1) if the null hypothesis in (2.4) is satisfied, then we have

$$\limsup_{n \rightarrow \infty} \mathbb{P}(\hat{d}_\infty < \hat{q}_\alpha^*) \leq \alpha.$$

(2) if the null hypothesis in (2.4) is satisfied and the set

$$\mathcal{E} = \{d \in \mathcal{D} : |\mu_1(d, \beta_1) - \bar{\mu}(d, \beta)| = d_\infty\}$$

consists of one point, then we have

$$\lim_{n \rightarrow \infty} \mathbb{P}(\hat{d}_\infty < \hat{q}_\alpha^*) = \begin{cases} 0, & d_\infty > \Delta, \\ \alpha, & d_\infty = \Delta. \end{cases}$$

(3) if the alternative hypothesis in (2.4) is satisfied, then we have

$$\lim_{n \rightarrow \infty} \mathbb{P}(\hat{d}_\infty < \hat{q}_\alpha^*) = 1.$$

Next, we establish a similar result for the test (2.14). For this purpose we introduce the random variable

$$S := \max \left\{ \max_{(i,d) \in \tilde{\mathcal{E}}^+} G((i,d)), \max_{(i,d) \in \tilde{\mathcal{E}}^-} -G((i,d)) \right\}, \quad (5.4)$$

where

$$\tilde{\mathcal{E}}^\pm := \{(i,d) \in \{1, \dots, m\} \times \mathcal{D} : \mu_i(d, \beta_i) - \bar{\mu}(d, \beta) = \pm d_{\infty, \infty}\},$$

the process $G = \{G((i,d))\}_{(i,d) \in \{1, \dots, m\} \times \mathcal{D}}$ is defined by

$$G((i,d)) := \left(\frac{\partial(\mu_i(d, b_i) - \bar{\mu}(d, b))}{\partial b} \right)^T \Big|_{b=\beta} Z, \quad i \in \{1, \dots, m\}, d \in \mathcal{D}$$

and Z is the centered γ -dimensional normal distributed random variable defined in (5.2).

Theorem 6.2. *Let Assumptions 1-3 be satisfied and assume that the random variable S in (5.4) has a continuous distribution function. Furthermore, let $\alpha \in (0, 1)$ be small enough, such that the α -quantile of S is negative. Then the test defined by (2.14) for the hypotheses (2.11) is consistent and has asymptotic level α . More precisely,*

(1) if the null hypothesis in (2.11) is satisfied, then we have

$$\limsup_{n \rightarrow \infty} \mathbb{P}(\hat{d}_{\infty, \infty} < \hat{q}_{\alpha, \infty}^*) \leq \alpha.$$

(2) if the null hypothesis in (2.11) is satisfied and the set

$$\tilde{\mathcal{E}} = \{(i, d) \in \{1, \dots, m\} \times \mathcal{D} : |\mu_i(d, \beta_i) - \bar{\mu}(d, \beta)| = d_{\infty, \infty}\}$$

consists of one point, then we have

$$\lim_{n \rightarrow \infty} \mathbb{P}(\hat{d}_{\infty, \infty} < \hat{q}_{\alpha, \infty}^*) = \begin{cases} 0, & d_{\infty, \infty} > \Delta, \\ \alpha, & d_{\infty, \infty} = \Delta. \end{cases}$$

(3) if the alternative hypothesis in (2.11) is satisfied, then we have

$$\lim_{n \rightarrow \infty} \mathbb{P}(\hat{d}_{\infty, \infty} < \hat{q}_{\alpha, \infty}^*) = 1.$$

6.2 Proof of Theorem 6.1

6.2.1 A preliminary result

We begin with a preliminary result, which is the basic ingredient for the proof of Theorem 6.1.

Theorem 6.3. *Let Assumptions 1-3 be satisfied. Then, as $n_1, \dots, n_k \rightarrow \infty$, the statistic \hat{d}_{∞} defined in (2.5) satisfies*

$$\sqrt{n}(\hat{d}_{\infty} - d_{\infty}) \xrightarrow{d} T,$$

where the random variable T is defined in (5.1).

Proof. The proof is conducted in four steps. First, observe that under Assumptions 1-3 the maximum likelihood estimate $\hat{\beta}$ defined in (2.6) satisfies $\sqrt{n}(\hat{\beta} - \beta) \xrightarrow{d} Z$, where $Z \sim \mathcal{N}_{\gamma}(0, \Sigma)$ with covariance matrix Σ defined by (5.3).

Second, similar arguments as given for the proof of the process convergence in equation (A.7) of Dette et al. (2018) show the weak convergence of the process

$$\sqrt{n} \left\{ (\mu_1(d, \hat{\beta}_1) - \bar{\mu}(d, \hat{\beta})) - (\mu_1(d, \beta_1) - \bar{\mu}(d, \beta)) \right\}_{d \in \mathcal{D}} \xrightarrow{d} \{G(d)\}_{d \in \mathcal{D}}$$

in the space $\ell^\infty(\mathcal{D})$ of bounded real-valued functions on \mathcal{D} equipped with the supremum-norm $\|\cdot\|_\infty$, where G is the Gaussian process defined in (5.2). Third, note that the mapping

$$\|\cdot\|_\infty : \begin{cases} \ell^\infty(\mathcal{D}) & \rightarrow \mathbb{R}, \\ g & \rightarrow \|g\|_\infty = \sup_{d \in \mathcal{D}} |g(d)| \end{cases}$$

is directionally Hadamard differentiable with respect to $(\ell^\infty(\mathcal{D}), \|\cdot\|_\infty)$ with directional Hadamard derivative at $g_0 \in \ell^\infty(\mathcal{D})$ given by

$$D_{g_0} : \begin{cases} \ell^\infty(\mathcal{D}) & \rightarrow \mathbb{R}, \\ g & \rightarrow D_{g_0}(g) = \max\{\max_{d \in \mathcal{E}^+} g(d), \max_{d \in \mathcal{E}^-} -g(d)\} \end{cases}, \quad (5.5)$$

where $\mathcal{E}^\pm := \{d \in \mathcal{D} : g_0(d) = \pm \|g_0\|_\infty\}$ (see Cárcamo et al. (2020), Theorem 2.1). Fourth, we apply the delta method for directionally Hadamard differentiable functions (see Shapiro (1991), Theorem 2.1) to complete the proof. \square

6.2.2 Proof of Theorem 6.1

Let $\mathcal{Y} = \{Y_{\ell ij} | i = 1, \dots, n_{\ell j}, j = 1, \dots, r, \ell = 1, \dots, k\}$ denote the data and define the functions

$$g(d) := \mu_1(d, \beta_1) - \bar{\mu}(d, \beta),$$

$$\hat{g}(d) := \mu_1(d, \hat{\beta}_1) - \bar{\mu}(d, \hat{\beta}),$$

$$\hat{g}^*(d) := \mu_1(d, \hat{\beta}_1^*) - \bar{\mu}(d, \hat{\beta}^*)$$

and the corresponding maximum deviations $\hat{d}_\infty^* := \|\hat{g}^*\|_\infty$ and $\hat{d}_\infty := \|\hat{g}\|_\infty$. Similar arguments as given for the proof of (A.25) in Dette et al. (2018) yield the process convergence

$$\sqrt{n}(\hat{g}^* - \hat{g}) \xrightarrow{d} \{G(d)\}_{d \in \mathcal{D}}$$

conditionally on \mathcal{Y} in probability which implies

$$\tilde{T}_n^* := D_g(\sqrt{n}(\hat{g}^* - \hat{g})) \xrightarrow{d} D_g(G) \stackrel{d}{=} T, \quad (5.6)$$

by the continuous mapping theorem, where D_g denotes the directional Hadamard derivative (5.5) at the function g . Moreover, we have

$$\begin{aligned}\sqrt{n}(\hat{d}_\infty - d_\infty) &= D_g(\sqrt{n}(\hat{g} - g)) + o_{\mathbb{P}}(1), \\ \sqrt{n}(\hat{d}_\infty^* - d_\infty) &= D_g(\sqrt{n}(\hat{g}^* - g)) + o_{\mathbb{P}}(1).\end{aligned}$$

Then, subtracting the first equation from the second and using sub-additivity of the directional Hadamard derivative yields

$$\sqrt{n}(\hat{d}_\infty^* - \hat{d}_\infty) \leq \tilde{T}_n^* + o_{\mathbb{P}}(1), \quad (5.7)$$

where there is equality if the set \mathcal{E} consists of a single point (note that in this case the directional Hadamard derivative is linear). Building on these results we can derive part (1) and (2) of Theorem 6.1. In the case $d_\infty > \Delta$, note that

$$\mathbb{P}(\hat{d}_\infty < \hat{q}_\alpha^*) = \mathbb{P}(\hat{d}_\infty < \hat{q}_\alpha^*, \hat{d}_\infty \geq \Delta) + \mathbb{P}(\hat{d}_\infty < \hat{q}_\alpha^*, \hat{d}_\infty < \Delta),$$

where the first probability converges to zero, which follows by similar arguments as given on page 727 in Dette et al. (2018). The second term converges to zero, since, by Theorem 6.3, $\hat{d}_\infty \xrightarrow{\mathbb{P}} d_\infty > \Delta$. In the case $d_\infty = \Delta$, note that

$$\mathbb{P}(\hat{d}_\infty < \hat{q}_\alpha^*) = \mathbb{P}(\hat{d}_\infty < \hat{q}_\alpha^*, \hat{d}_\infty = \Delta) + \mathbb{P}(\hat{d}_\infty < \hat{q}_\alpha^*, \hat{d}_\infty > \Delta),$$

where the first probability sequence is asymptotically bounded above by (or equal to) α , because of (5.6) and (5.7) and the second probability sequence converges to zero, since $q_\alpha < 0$. Finally, in the case $d_\infty < \Delta$ statement (3) follows by the same arguments as given for the proof of (3.18) in Theorem 2 in Dette et al. (2018).

6.3 Proof of Theorem 6.2

The proof is analogous to the proof of Theorem 6.1 and only needs some additional adjustments. We start by deriving the asymptotic error distribution of the estimator $\hat{d}_{\infty, \infty}$.

6.3.1 A preliminary result

Theorem 6.4. *Let Assumptions 1-3 be satisfied. Then, as $n_1, \dots, n_k \rightarrow \infty$, the statistic $\hat{d}_{\infty, \infty}$ defined in (2.10) satisfies*

$$\sqrt{n}(\hat{d}_{\infty, \infty} - d_{\infty, \infty}) \xrightarrow{d} S,$$

where the random variable S is defined in (5.4).

Proof. We can copy the proof of Theorem 6.3 and only need to change the second and third step, the first and fourth step can be left unchanged. To this end, only note that by the functional delta method

$$\sqrt{n} \left\{ (\mu_i(d, \hat{\beta}_i) - \bar{\mu}(d, \hat{\beta})) - (\mu_i(d, \beta_i) - \bar{\mu}(d, \beta)) \right\}_{(i,d) \in \{1, \dots, m\} \times \mathcal{D}} \xrightarrow{d} \{G((i, d))\}_{(i,d) \in \{1, \dots, m\} \times \mathcal{D}}$$

holds true in the space $\ell^\infty(\{1, \dots, m\} \times \mathcal{D})$ of bounded real-valued functions on $\{1, \dots, m\} \times \mathcal{D}$ equipped with the supremum-norm

$$\|g\|_\infty = \sup_{(i,d) \in \{1, \dots, m\} \times \mathcal{D}} |g(i, d)|$$

and that the supremum-norm is directionally Hadamard differentiable on the space $\ell^\infty(\{1, \dots, m\} \times \mathcal{D})$ with derivative at g_0 given by

$$D_{g_0} : \begin{cases} \ell^\infty(\{1, \dots, m\} \times \mathcal{D}) & \rightarrow \mathbb{R}, \\ g & \rightarrow D_{g_0}(g) = \max\{\max_{(i,d) \in \mathcal{E}^+} g(i, d), \max_{(i,d) \in \mathcal{E}^-} -g(i, d)\} \end{cases},$$

where $\mathcal{E}^\pm := \{(i, d) \in \{1, \dots, m\} \times \mathcal{D} : g_0(i, d) = \pm \|g_0\|_\infty\}$.

□

6.3.2 Proof of Theorem 6.2

Defining the processes $g((i, d)) := \mu_i(d, \beta_i) - \bar{\mu}(d, \beta)$, $\hat{g}((i, d)) := \mu_i(d, \hat{\beta}_i) - \bar{\mu}(d, \hat{\beta})$, $\hat{g}^*((i, d)) := \mu_i(d, \hat{\beta}_i^*) - \bar{\mu}(d, \hat{\beta}^*)$ as well as $\hat{d}_{\infty, \infty}^* := \|\hat{g}^*\|_\infty$ and $\hat{d}_{\infty, \infty} := \|\hat{g}\|_\infty$ over the set $\{1, \dots, m\} \times \mathcal{D}$, we can use the same arguments as given in the proof of Theorem 6.1, where we employ Theorem 6.4 instead of Theorem 6.3.

References

- Bean, N. W., Ibrahim, J. G., and Psioda, M. A. (2023). Bayesian multiregional clinical trials using model averaging. *Biostatistics*, 24(2):262–276.
- Biesheuvel, E. and Hothorn, L. A. (2002). Many-to-one comparisons in stratified designs. *Biometrical Journal*, 44(1):101–116.
- Bornkamp, B., Pinheiro, J., and Bretz, F. (2015). Dosefinding: Planning and analyzing dose finding experiments. *R-package version 1.0-2*. Available at <https://cran.r-project.org/web/packages/DoseFinding/index.html>.

- Bretz, F., Möllenhoff, K., Dette, H., Liu, W., and Trampisch, M. (2018). Assessing the similarity of dose response and target doses in two non-overlapping subgroups. *Statistics in Medicine*, 37(5):722–738.
- Bretz, F., Pinheiro, J. C., and Branson, M. (2005). Combining multiple comparisons and modeling techniques in dose-response studies. *Biometrics*, 61(3):738–748.
- Cade, B. S. (2011). Estimating equivalence with quantile regression. *Ecological Applications*, 21(1):281–289.
- Cárcamo, J., Cuevas, A., and Rodríguez, L.-A. (2020). Directional differentiability for supremum-type functionals: Statistical applications. *Bernoulli*, 26(3):2143 – 2175.
- Chiang, C. and Hsiao, C.-F. (2019). Use of interval estimations in design and evaluation of multiregional clinical trials with continuous outcomes. *Statistical Methods in Medical Research*, 28(7):2179–2195.
- Dette, H., Möllenhoff, K., Volgushev, S., and Bretz, F. (2018). Equivalence of regression curves. *Journal of the American Statistical Association*, 113(522):711–729.
- Gsteiger, S., Bretz, F., and Liu, W. (2011). Simultaneous confidence bands for nonlinear regression models with application to population pharmacokinetic analyses. *Journal of Biopharmaceutical Statistics*, 21(4):708–725.
- ICH (2017). International Conference on Harmonisation Tripartite Guidance E17 on General Principles for Planning and Design of Multi-Regional Clinical Trials.
- Kaneko, S. (2023). A method for ensuring a consistent dose–response relationship between an entire population and one region in multiregional dose–response studies using mcp-mod. *Statistics in Biopharmaceutical Research*, 0(0):1–9.
- Kim, J. H., Robinson, and P., A. (2019). Interval-based hypothesis testing and its applications to economics and finance. *Econometrics*, 7(2).
- Lakens, D. and Delacre, M. (2020). Equivalence testing and the second generation p-value. *Meta-Psychology*, 4.
- Liao, J. J., Yu, Z., and Li, Y. (2018). Sample size allocation in multiregional equivalence studies. *Pharmaceutical Statistics*, 17(5):570–577.
- Liu, W., Bretz, F., Hayter, A. J., and Wynn, H. P. (2009). Assessing non-superiority, non-inferiority of equivalence when comparing two regression models over a restricted covariate region. *Biometrics*, 65(4):1279–1287.

- Liu, W., Hayter, A. J., and Wynn, H. P. (2007). Operability region equivalence: simultaneous confidence bands for the equivalence of two regression models over restricted regions. *Biometrical Journal*, 49(1):144–150.
- Möllenhoff, K., Bretz, F., and Dette, H. (2020). Equivalence of regression curves sharing common parameters. *Biometrics*, 76(2):518–529.
- Möllenhoff, K., Dette, H., and Bretz, F. (2021). Testing for similarity of binary efficacy and toxicity responses. *Biostatistics*, 23(3):949–966.
- Ollier, A., Zohar, S., Morita, S., and Ursino, M. (2021). Estimating similarity of dose-response relationships in phase i clinical trials—case study in bridging data package. *International Journal of Environmental Research and Public Health*, 18(4):1639.
- Ostrovski, V. (2022). Testing equivalence to power law distributions. *Statistics & Probability Letters*, 181:109287.
- Pinheiro, J., Bornkamp, B., and Bretz, F. (2006). Design and analysis of dose-finding studies combining multiple comparisons and modeling procedures. *Journal of Biopharmaceutical Statistics*, 16(5):639–656.
- Rose, E. M., Mathew, T., Coss, D. A., Lohr, B., and Omland, K. E. (2018). A new statistical method to test equivalence: an application in male and female eastern bluebird song. *Animal Behaviour*, 145:77–85.
- Shapiro, A. (1991). Asymptotic analysis of stochastic programs. *Annals of Operations Research*, 30(1):169–186.
- Song, S. Y., Chee, D., and Kim, E. (2019). Strategic inclusion of regions in multiregional clinical trials. *Clinical Trials*, 16(1):98–105.
- Sonnemann, E. (2008). General solutions to multiple testing problems. *Biometrical Journal*, 50(5):641–656.
- Teng, Z., Lin, J., and Zhang, B. (2018). Practical recommendations for regional consistency evaluation in multi-regional clinical trials with different endpoints. *Statistics in Biopharmaceutical Research*, 10(1):50–56.
- Thomas, N. (2006). Hypothesis testing and Bayesian estimation using a sigmoid *emax* model applied to sparse dose-response designs. *Journal of Biopharmaceutical Statistics*, 16(5):657–677.
- Wellek, S. (2010). *Testing Statistical Hypotheses of Equivalence and Noninferiority*. CRC Press.

Yamaguchi, Y. and Sugitani, T. (2021). Sample size allocation in multiregional dose-finding study using mcp-mod. *Statistics in Biopharmaceutical Research*, 13(4):395–404.